

Lynx: New Tool to Model Mode-I Fatigue Crack Propagation

R. Branco¹, F.V. Antunes² and J.D.M. Costa²

¹ CEMUC, Department of Mechanical Engineering, ISEC, Polytechnic Institute of Coimbra, Rua Pedro Nunes, Quinta da Nora, 3030-199 Coimbra, Portugal.

rbranco@isec.pt

² CEMUC, Department of Mechanical Engineering, University of Coimbra, Rua Luís Reis Santos, Pólo II, 3030-788 Coimbra, Portugal.

fernando.ventura@dem.uc.pt; jose.domingos@dem.uc.pt

ABSTRACT. *The objective here is to present new software to simulate in-plane fatigue crack propagation. This computer application, named Lynx, incorporates fifteen different notched and unnotched geometries with through cracks, surface cracks and corner cracks. An intuitive and user-friendly interface to simplify the input data was developed. Default values can be used to minimise the learning curve of less experienced users. Although simple, Lynx has been used to address different research questions. Finally, an application example of fatigue crack propagation in notched and unnotched plates is examined in order to provide an overview of the main capabilities of the proposed tool.*

INTRODUCTION

Modern defect-tolerant design approaches to fatigue are based on the premise that engineering structures are inherently flawed, i.e., manufacturing defects are potentially present. Therefore, accurate tools to predict the crack shape evolution as well as the fatigue life are fundamental to increase the reliability of mechanical components and structures.

The application of numerical methods to study fatigue crack growth (FCG) problems have proved to be extremely useful. One of the most efficient approaches consists of an automatic iterative procedure based on the finite element method (FEM) that comprises three main steps repeated cyclically: firstly, a representative 3D-FE model is created; secondly, the stress intensity factor for the cracked body is calculated; and thirdly, the crack advances can be calculated integrating the Paris law from which the new crack front is obtained.

Regarding the definition of the new crack front, two main methodologies can be distinguished. The two degree freedom model considers only two crack front key points and assumes a particular crack shape throughout the propagation [1-2]. Due to this fact, it is not suitable for situations containing irregular crack shapes or cases with significant shape variations. In such cases, the multiple degree freedom model [3-5] is preferable

because each crack front node is studied separately without imposing constraints on crack shape.

The modelling of FCG problems using commercial FEM packages is, in general, time consuming and laborious. On this regard, different software solutions have been developed to avoid this problem [6-9]. Additionally, sophisticated algorithms to analyse FCG problems in 3D cracked geometries, based on structured and unstructured meshes, have also been proposed [10-12]. Nevertheless, most of the existing software are not available commercially and have been used for research purposes.

In this article, new software to simulate in-plane fatigue crack propagation is presented. Fifteen different notched and unnotched geometries that include plates, round bars and rectangular bars with through cracks, surface cracks and corner cracks are available. An intuitive and user-friendly interface was developed in order to improve its functionality and simplicity. For less experienced users, default values are proposed in order to simplify all tasks associated with the numerical modelling definition. Finally, an application example of fatigue crack propagation in notched and unnotched plates is examined to provide an overview of the main capabilities of the proposed tool.

LYNX: IN-PLANE FCG SOFTWARE

Lynx is modular software designed to address in-plane FCG problems without requiring significant modelling. The computer application incorporates fifteen generic geometries often studied in this context. Some examples are exhibited in Figure 1. It encompasses through cracks (Figures 2a-2c), surface cracks (Figures 2d-2f) and corner cracks (Figures 2g-2j). Several geometries include lateral notches (Figures 2b, 2d, 2f, 2h, 2j). In the cases of Figures 2d-2j, automatic transitions from surface or corner crack to through cracks are carried out.

The computer application was created using the Visual Basic language. The algorithm of calculation is presented in Figure 2 and comprises a pre-processing stage, a processing stage and a post-processing stage. The pre-processing stage is devoted to the input data, namely geometry dimensions, crack front coordinates, material properties,

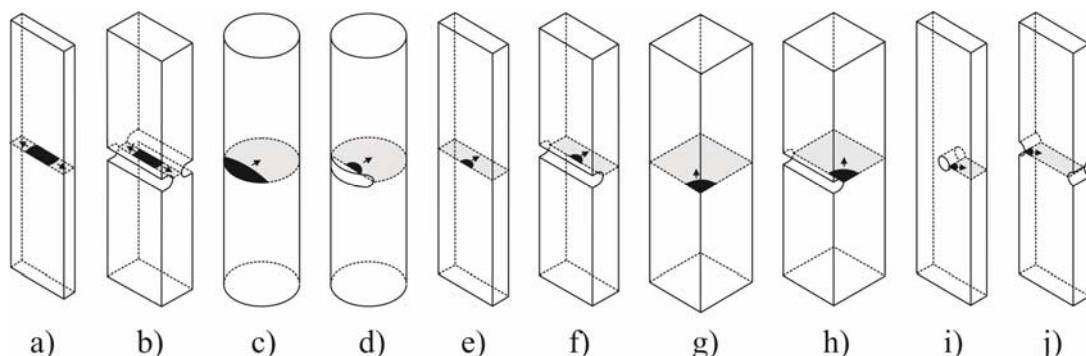


Figure 1. Typical examples of cracked geometries included in Lynx.

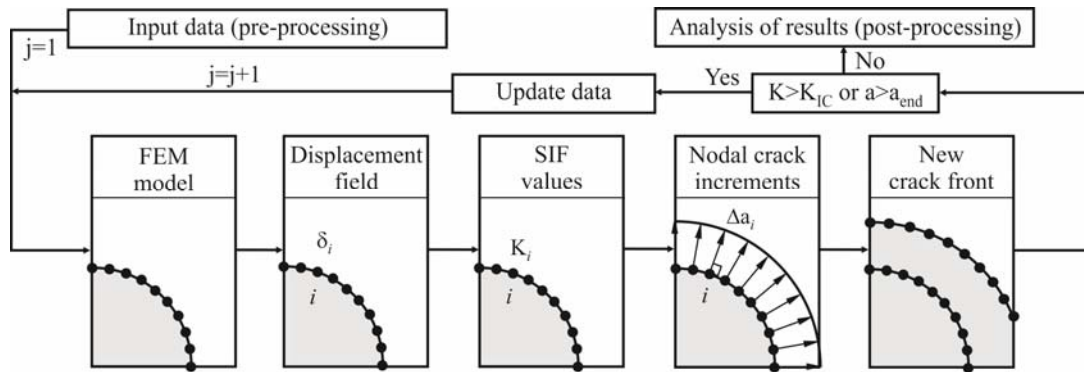


Figure 2. Schematic illustration of calculation procedure.

loading definitions, mesh options, propagation parameters and method of SIF calculation. In order to simplify these definitions, an intuitive user-friendly graphical user interface (GUI) was provided. The interface consists of eight windows hierarchically organised according to the type of input data. This approach is more attractive for the user since it simplifies the input data process and ensures an appropriate separation of tasks. Besides, enlightening drawings were added as a means of increasing the understanding of the problem. Default values are also suggested which can minimise the learning curve of less experienced users.

Figure 3 shows three windows of the graphical user interface. Briefly, window 1 (Figure 3a) is used to select the geometry and its dimensions; window 2 allows defining the crack front up to fifty corner nodes; window 3 (Figure 3b) can be used to insert the material properties (such as elastic constants, fracture toughness, fatigue crack growth rates, etc.) and type and magnitude of loading; in window 4 (Figure 3c) are specified the mesh details, i.e. number and radial size of concentric rings surrounding the crack front, and the total number of elements of the model; in window 5, the SIF calculation method is selected; in window 6 is possible to define the maximum crack growth increment as well as to select the type of crack front definition (by a polyline or by a cubic spline) and the position of mid-side nodes of elements surrounding the crack tip (at quarter-positions or not); in window 7, the variables needed to carry out an automatic transition from surface or corner cracks to through cracks (cases of figures 2d-2j) are specified; and finally, in window 8, several output options are taken in order to ensure a fast analysis of desired results and an adequate management of temporary files created during the simulation. Besides, it is important to note that for each crack front, different Paris law constants can be defined, and therefore, crack closure can be included in the models. The Paris law constants can also be changed automatically during the crack transition from surface and corner crack to through cracks enabling the use of different FCG rates.

The processing stage (Figure 2) is the core of fatigue crack growth simulation and comprises five steps repeated successively. Firstly, a numerical model representative of the problem is created. At this moment, the FE model generated is compatible with the commercial FE package Cosmos/M. Nevertheless, due to the modularity of Lynx, other

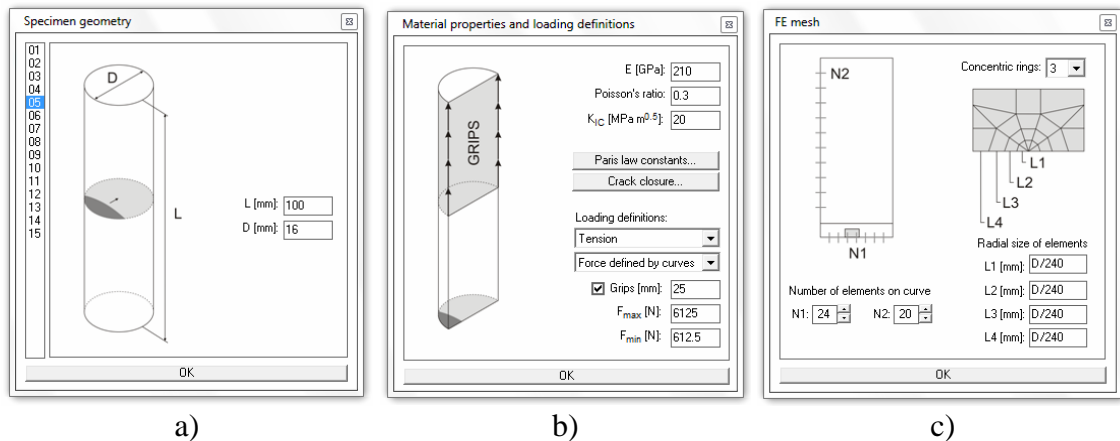


Figure 3. Typical windows of Lynx interface: a) window 1; b) window 3; c) window 4.

plug-in programs can be developed. Secondly, the displacements (δ_i) of crack front nodes are calculated by performing a linear elastic analysis. Thirdly, the stress intensity factors (K_i) along the crack front are computed using matching extrapolation methods. Fourthly, an adequate crack growth model is applied in order to define the crack front advances (Δa_i) with which a new provisional crack front is established. Finally, the positions of corner nodes of crack front are relocated to their definitive positions.

The post-processing stage is designed to provide a faster analysis of results. Data can be exported to template files which characterise, among other variables, the evolution of crack front, the number of fatigue cycles and the evolution of stress intensity factors along the crack front. Moreover, it is also possible to complement the analysis with graphical and numerical results by using the post-processor GeoStar.

APPLICATION EXAMPLE

The application example presented here concerns the fatigue crack growth of unnotched and notched plates (Figures 2a and 2b, respectively). The geometry of Figure 2a consists of a M(T) specimen geometry characterised by a height ($2H$), width ($2W$) and thickness (t). The geometry of Figure 2b is a M(T) specimen modified with lateral U-shaped grooves and is characterised by a height ($2H$), width ($2W$), groove depth (b), groove radius (r), original thickness (t_0) and reduced thickness ($t=t_0-2b$). The crack is normal to the axis of specimen and is placed at its middle section. The material simulated was the DIN 34CrNiMo6, which was assumed to be homogeneous, isotropic and linear elastic with $\nu=0.296$ and $E=209.8$ GPa [13]. Due to material, loading and geometry symmetries, only a one-eighth of the specimens were modelled.

The typical FE meshes used, either for unnotched or notched geometries, are exhibited in Figure 4. The meshes were created with the 20-node and the 20-node collapsed isoparametric hexahedric elements, having about 10370 elements and 116020 nodes. Singular elements with mid-side nodes at quarter point positions were considered

around the crack front. A spider web pattern, made of three concentric rings centred at the crack tip, was created (Figure 4d). A smooth change from a refined mesh near the crack front to a larger one at remote positions was carried out (Figure 4c) in order to reduce the computational effort. Along the thickness, the mesh was designed with an increasing level of refinement (Figures 4b and 4d). The refinement was important to resolve the stress gradient existing in this direction, namely near the corner points of the crack front [14]. It has a total of 50 layers divided into three main regions (Figure 4d). The most refined one (I), located near the surface, had 26 layers non-uniformly distributed with a minimum element size of $1\mu\text{m}$. The intermediate region (II) had 14 layers uniformly distributed with element sizes of $50\mu\text{m}$. The larger region (III) had 10 layers disposed uniformly, whose element size depends on the specimen thickness.

The radial size of crack front elements (L_1 defined in Figure 4d) was maintained constant ($W/375$). Regarding K calculation, the direct method of extrapolation with two points was employed [15]. The crack front advances were computed using the Paris law, considering $C=2.42\times 10^{-8}$ and $m=2.56$ (ΔK in $\text{MPa m}^{0.5}$ and da/dN in mm/cycle). The maximum crack growth increment (Δa_{max}) was limited to less than $W/300$.

Figure 5 presents typical fatigue crack shape developments obtained with the present computer application for different situations. Figure 5a compares the crack shape evolution for an unnotched geometry and a notched geometry for the same thickness in the crack plane ($t=5\text{mm}$). In the unnotched case, the crack shape is almost straight except near the surface where a delay (d_1) is observed. In the other case, the crack growth along the boundary of the specimen is faster than in depth (d_2) due to the increase in stress concentration factor caused by the U-shaped groove. Figure 5b compares the crack shape evolution for two different thicknesses. The crack shape is almost straight in both situations except near the surface. Nevertheless, the delay near the surface increases with thickness, as can be seen by d_3 (which quantifies the difference between the surface coordinates of two crack fronts having the same length in depth). Besides, the extent of this region in thickness direction also increases with

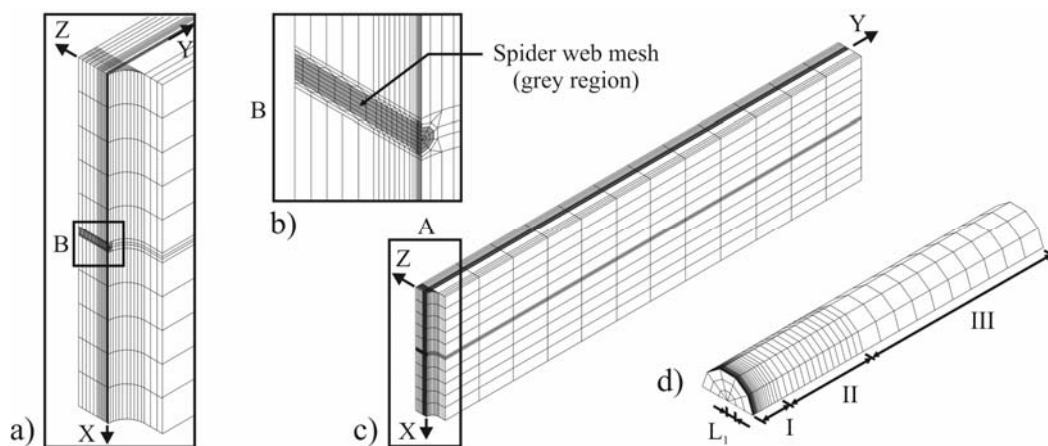


Figure 4. Finite element mesh of the U-shaped notched geometry ($2H=200\text{mm}$; $2W=50\text{mm}$; $r=1.5\text{mm}$; $b=3.0\text{mm}$, $t=5\text{mm}$)

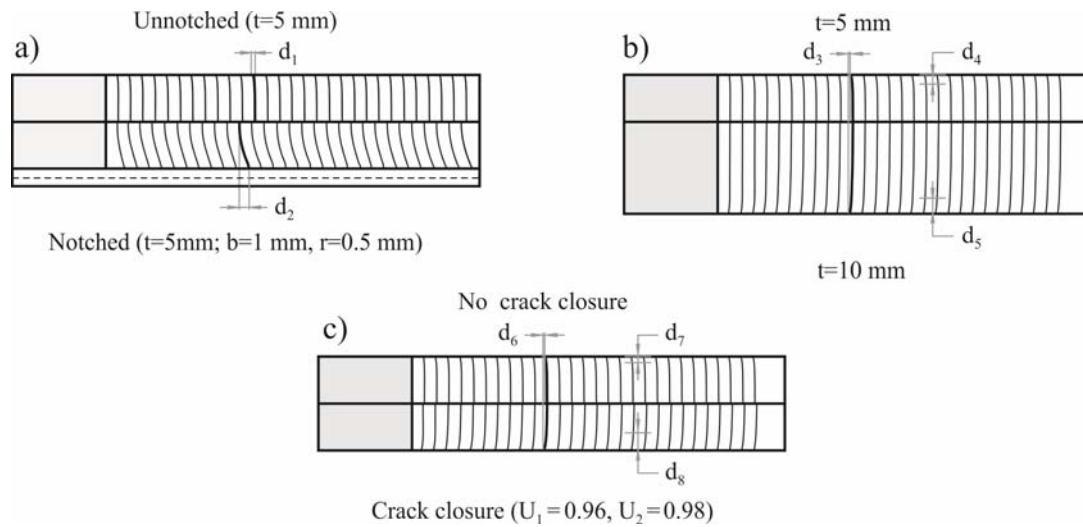


Figure 5. Effect of: a) notch; b) thickness; c) crack closure on fatigue crack shape evolution ($2H=200\text{mm}$; $2W=50\text{mm}$).

thickness, as can be distinguished by comparing both values of d_4 and d_5 . Figure 5c exhibits the effect of crack closure on fatigue crack growth. The case at the top has no crack closure while the other have crack closure (U) at the first and second nodes from free surface equal to $U_1=0.96$ and $U_2=0.98$, respectively. The analysis of variables d_7 and d_8 shows that different portions of thickness are affected. Moreover, the crack curvature is clearly increased due to the presence of crack closure, as demonstrates the value of d_6 (which measures the difference between the surface coordinates of two crack fronts having the same length in depth).

A more feasible analysis of crack shape profiles is generally done using dependent parameters. Figure 6a plots the evolution of crack aspect ratio (d/t) against the dimensionless crack length (a/W) for different notched ($r=1.5\text{mm}$, $b=2\text{mm}$, $t=5\text{mm}$) and unnotched cases. Different initial crack shapes were considered (b_0/t_0). Stable propagations (with a constant- K) for the notched and unnotched cases were also included. As can be seen, at the early propagation stage, a high sensitivity of the crack aspect ratio with regard to the initial crack configuration is observed. Significant crack shape modifications occur in this period. Nevertheless, this high dependence on initial crack shape weakens gradually leading the crack shape to preferred propagation paths (PPP). The convergence is faster for initial crack configurations closer to the PPP.

Figure 6b shows the variation of K_{\min}/K_{\max} with the dimensionless crack length for notched ($r=1.5\text{mm}$, $b=2\text{mm}$, $t=5\text{mm}$) and unnotched ($t=5\text{mm}$) cases. The ratios of the stable propagations referred in the previous figure are also presented. As can be seen, both ratios are almost superimposed and are close the unity (≈ 0.98). Regarding the curved crack fronts, it is observed a sudden increase in the K_{\min}/K_{\max} ratio for values of $a/D < 0.3$. After that, regardless of the initial crack shape, the K_{\min}/K_{\max} ratios follow the iso- K values. This trends help to explain the more significant shape modifications occurred at the early propagation period, as previously observed in Figure 6a.

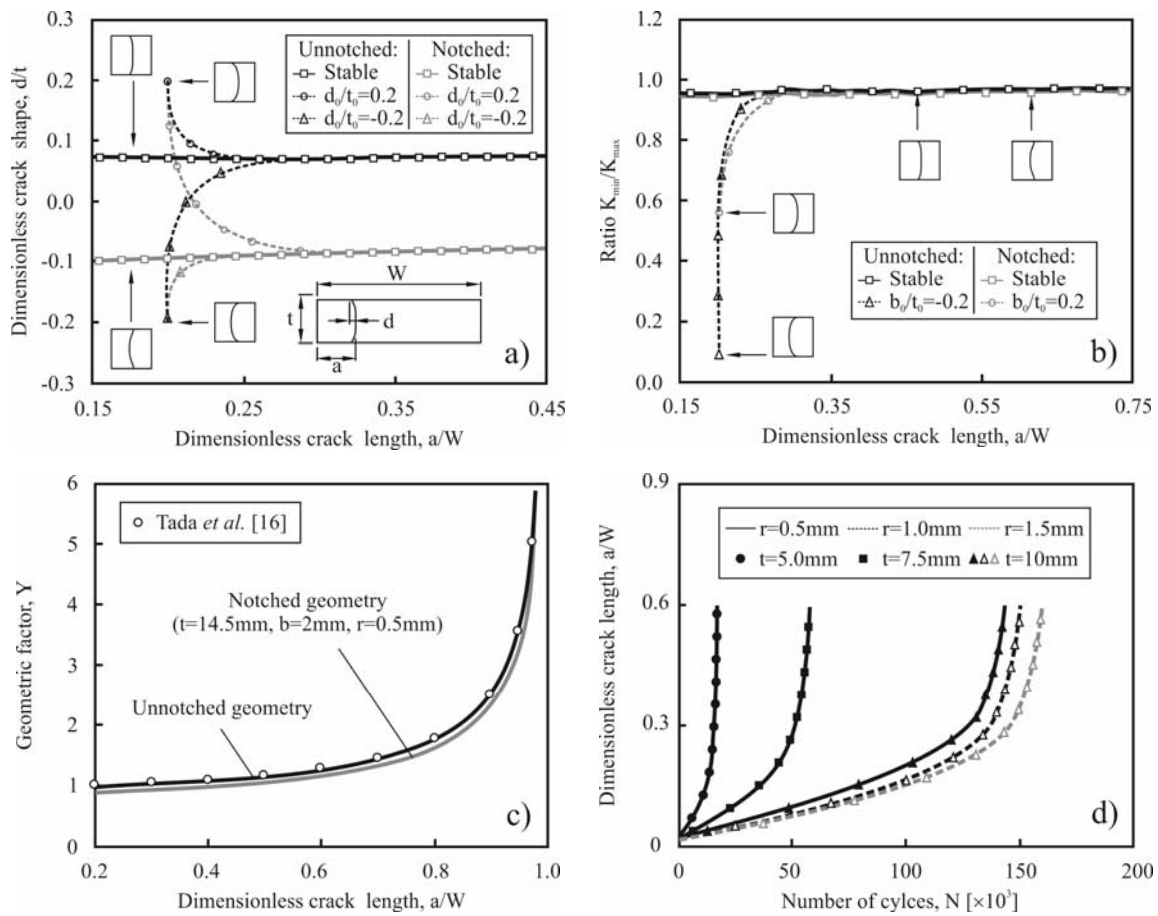


Figure 6. Evolution of: a) d/t with a/W ; b) K_{\min}/K_{\max} with a/W ; c) Y with a/W ; d) a/W with N ($2H=200\text{mm}$; $2W=50\text{mm}$).

Figure 6c exhibits the geometric factor (Y) for notched ($r=1.5\text{mm}$, $b=2\text{mm}$, $t=14.5\text{mm}$) and unnotched ($t=14.5\text{mm}$) geometries. The geometric factor derived from the SIF solution proposed in [16] is also plotted for the unnotched geometry. The values of Y for the unnotched geometry, obtained here and in [16], are very close, with differences lower than 3% for a/W within the range [0.2-0.9]. In the notched case, the lateral grooves are responsible for a reduction about 6.5% in the geometric factor.

The computer application can also be used to evaluate the number of fatigue cycles for different geometries. It can help designers to find the best design. Figure 6d plots the number of fatigue cycles (N) against the dimensionless crack length (a/W) for several notched geometries with initial straight cracks of 0.5 mm and $b=2\text{mm}$. Comparing the black full lines ($t=5\text{mm}$, $t=7.5\text{mm}$ and $t=10\text{mm}$), it is possible to conclude that the thickness has a determinant effect on the final life. Thicker specimens suffer lower stresses and, therefore, the resultant stress intensity factor is lower. Regarding the triangle series ($r=0.5\text{mm}$, $r=1.0$ and $r=1.5\text{mm}$), the increase in r , decreases the number of fatigue cycles. Smaller notch radii raise the stress concentration factors and consequently the crack tends to propagate faster.

CONCLUSIONS

A new tool to simulate in-plane FCG problems under mode-I loading was presented. It incorporates fifteen different major cracked geometries with which can be addressed a broad range of problems in the field of FCG. Due to its modular architecture more geometries and calculation algorithms can be added. An intuitive and user-friendly interface was developed to improve its functionality and simplicity. For less experienced users, default values are suggested to minimise the learning curve.

The computer application can be used to study the effects of different physical and material variables on crack shape evolution, stress intensity factors and fatigue life making it interesting to improve the design of mechanical components. Besides, the presented software can also be employed to optimise different numerical parameters, such as maximum crack advance, radial size of crack front elements, mesh topology and mesh density, etc.

ACKNOWLEDGEMENTS

The authors are indebted to FCT and FEDER for the financial support (Project PTDC/EME-PME/114892/2009; COMPETE: FCOMP-01-0124-FEDER-015171).

REFERENCES

1. Newman Jr., J.C., Raju, I.S. (1981) *Eng. Fract. Mech.* **15**, 185-192.
2. Carpinteri, A. (1992). *Fatigue Fract. Eng. Mater. Struct.* **15**, 1141-1153.
3. Smith, R.A., Cooper, J.F. (1989). *Int. Journal of Pressure Vessels and Piping* **36**, 315-326.
4. Lin, X.B., Smith, R.A. (1999) *Eng. Fract. Mech.* **63**, 503-522.
5. Branco, R., Antunes, F.V. (2008) *Eng. Fracture Mech.* **75**, 3020-3037.
6. Schöllmann, M., Fulland, M., Richard, H.A. (2003) *Eng. Fract. Mech.* **70**, 249-268.
7. Bremberg, D., Dhondt, G. (2008) *Eng. Fract. Mech.* **75**, 404-416.
8. Zencrack User's Manual v7.5 (2007) *Zentech International Limited*, UK.
9. Riddel, W., Ingraffea, A., Wawrzynek, P. (1997) *Eng. Fract. Mech.* **58**, 293-310.
10. Kolk, K., Kuhn, G. (2006) *Archive of Applied Mechanics* **76**, 699-709.
11. Ayhan, A. (2011) *Int. Journal of Solids and Structures* **48**, 492-505.
12. Weber, W., Steinmann P., Kuhn G. (2008) *Int. J. Fracture*, **149**, 175-192.
13. Branco, R., Costa, J.D., Antunes, F.V. (2012) *Theor. Appl. Fract. Mech.* (in press).
14. Branco, R., Antunes, F.V., Ricardo, L.C.H, Costa, J.D. (2012) *Finite Elem. Anal. Des.* **50**, 147-160.
15. Guinea, G.V., Planas, J., Elices, M. (2000). *Eng. Fract. Mech.* **66**, 243-255.
16. Tada, H., Paris P.C., Irwin G. (1973) *The stress analysis of cracks handbook*, Del Research Corporation, Missouri, USA.